

High-redshift radio galaxies with the International LOFAR Telescope (ILT)

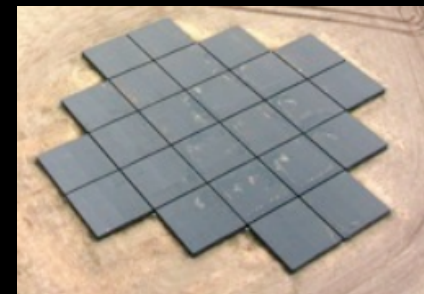
Presenter:
Marco Bondi
Organization:
INAF - IRA



1-2 March 2023
INAF/IRA Bologna

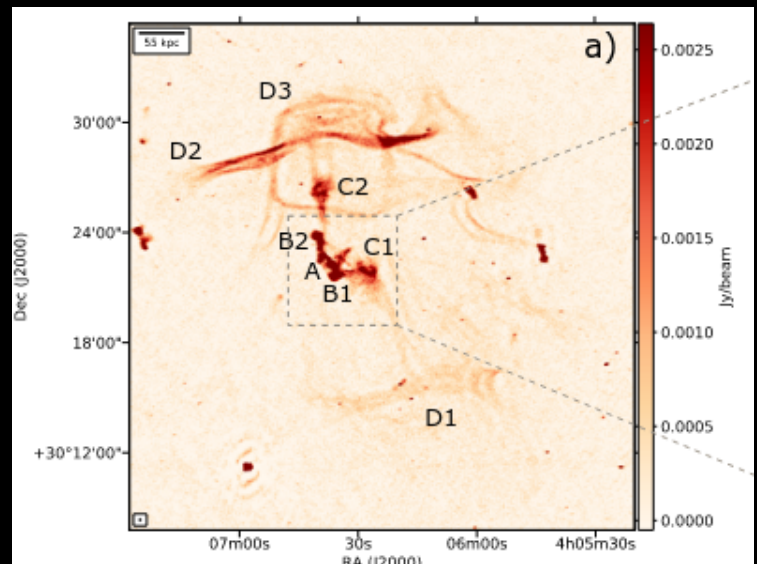
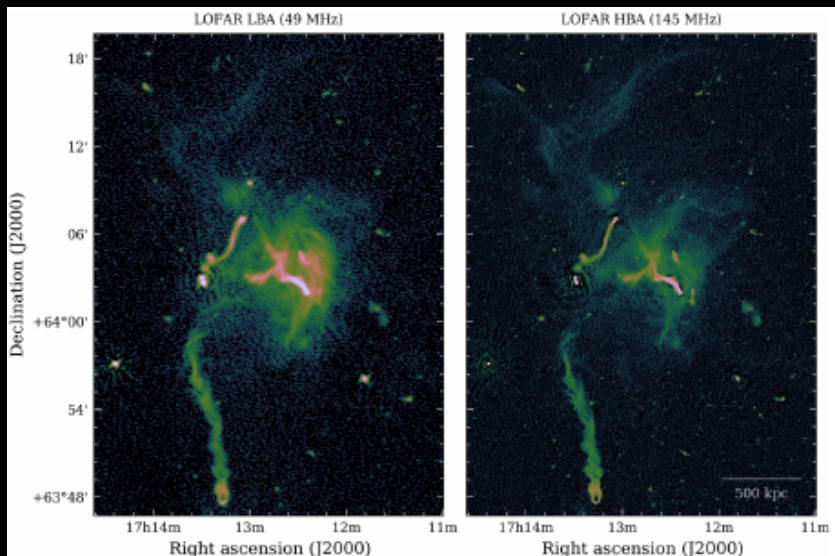
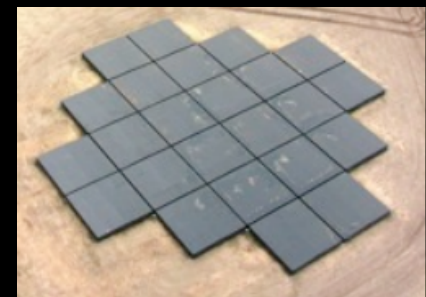
The Low Frequency Array (LOFAR)

- Low Band Antenna (LBA; ~50 MHz)
- High Band Antenna (HBA; ~144 Mhz)
- Core stations (24, baseline 0.15-3 km)
- Remote stations (14, baseline 5-100 km)
- HBA: 6" resolution, rms \sim 80 μ Jy (8 hrs)



The Low Frequency Array (LOFAR)

- Low Band Antenna (LBA; ~50 MHz)
- High Band Antenna (HBA; ~145 Mhz)
- Core stations (24, baseline 0.15-3 km)
- Remote stations (14, baseline 5-100 km)
- HBA: 6" resolution, rms $\sim 80 \mu\text{Jy}$ (8 hrs)

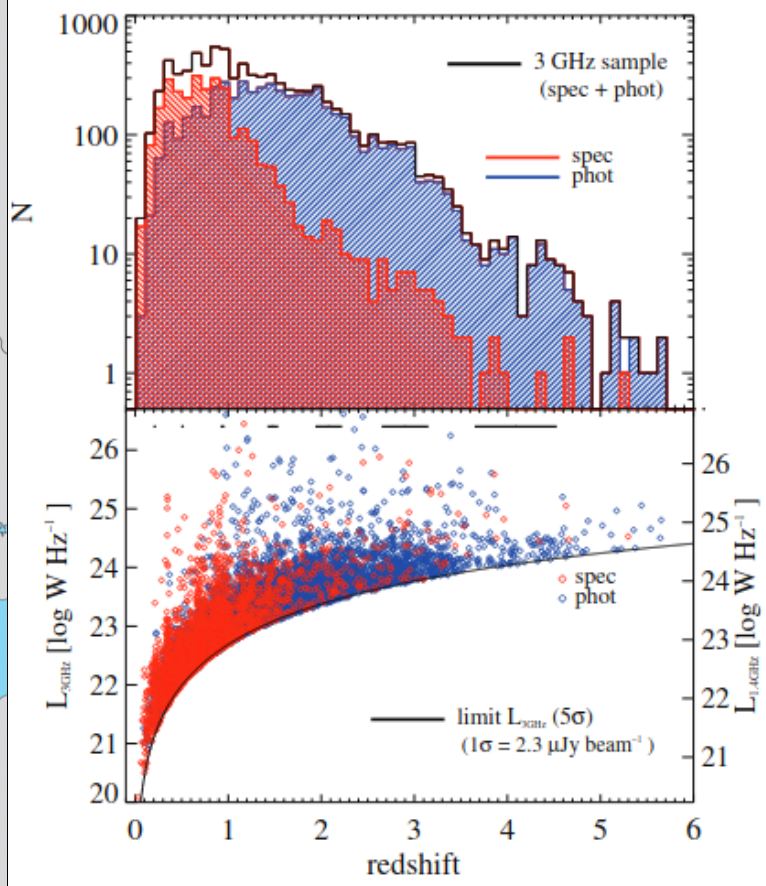


International LOFAR Telescope (ILT)

Resolution from 6" to 0.3"
At $z \sim 1$, from ~ 50 kpc to 2.5 Kpc



HBA: 144 MHz
38 Dutch stations
14 (+2) International stations: baselines up to ~ 2000 km

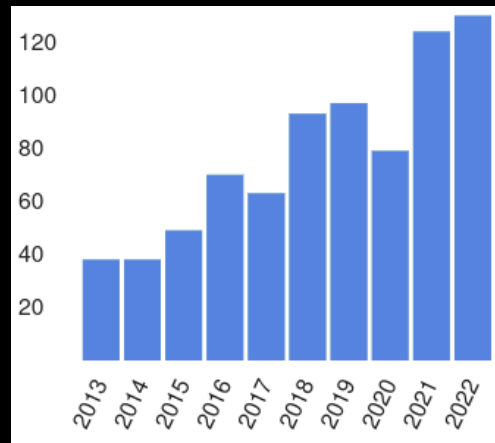


Delvecchio+2017

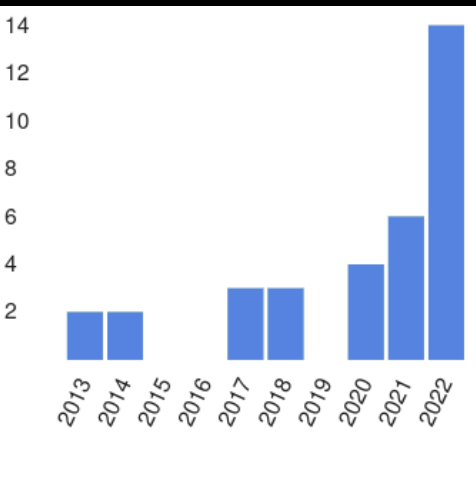
ILT Data Analysis: bottleneck

- **Premises:**

- All LOFAR obs include the International Stations (IS)
- Typically IS are **NOT** used



LOFAR papers 2013-2022

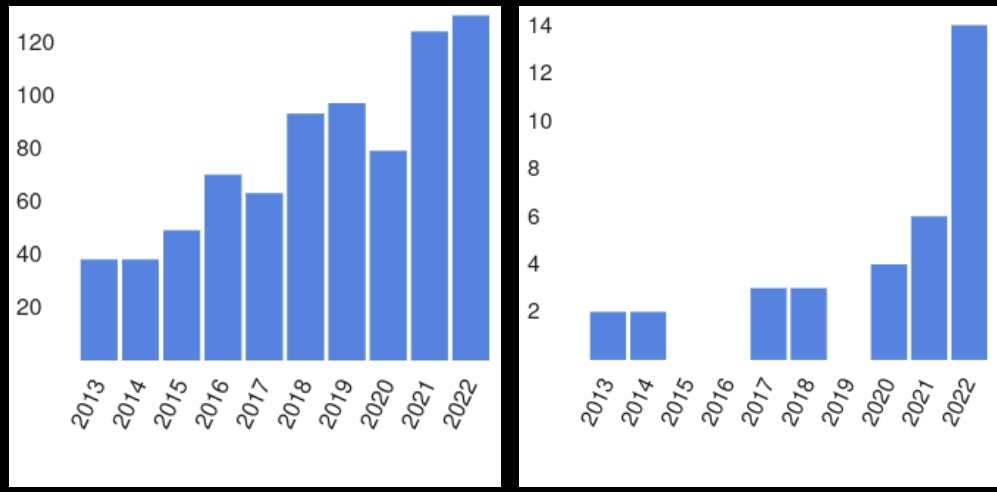


ILT papers 2013-2022

ILT Data Analysis: bottleneck

- **Premises:**

- All LOFAR obs include the International Stations (IS)
- Typically IS are **NOT** used



LOFAR papers 2013-2022

ILT papers 2013-2022

- **Issues:**

- Time and computer resources demanding
- A robust and reliable pipeline not available (until recently)

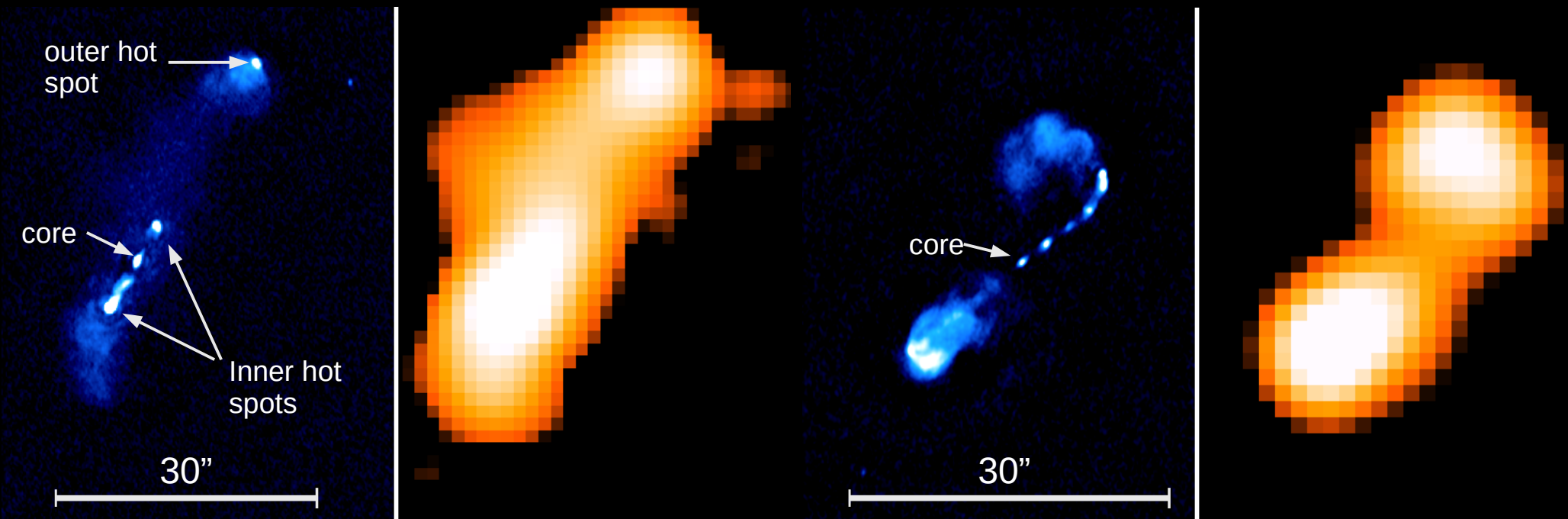
- **Solution:**

- Long baseline pipeline (Morabito+2022)

<https://github.com/lmorabit/lofar-vlbi/>

ILT images: Radio Galaxies at $z \geq 1$ in the NEP Deep Field

(Bondi+ in prep.)



$z=1.61$ $L_R = 6.7 \times 10^{27}$ W/Hz

ILT (48 hrs)
 $0''.45 \times 0''.31$
r.m.s ~ 18 μ Jy/beam
 $S_P = 40$ mJy/beam

LOFAR (72 hrs)
 $6''.0 \times 6''.0$
r.m.s = 41 μ Jy/beam
 $S_P = 150$ mJy/beam

$z=1.60$ $L_R = 4.7 \times 10^{27}$ W/Hz

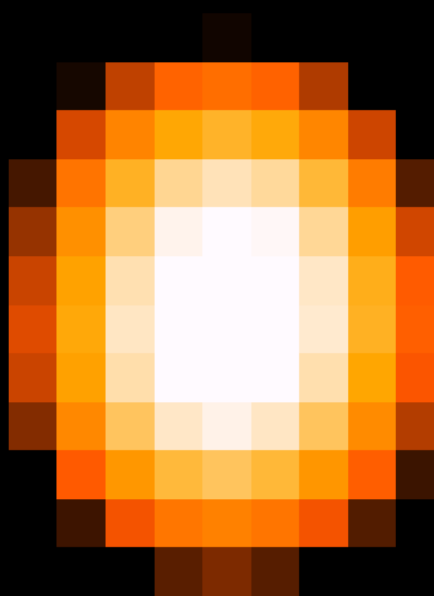
ILT (48 hrs)
 $0''.46 \times 0''.32$
r.m.s ~ 20 μ Jy/beam
 $S_P = 4.8$ mJy/beam

LOFAR (72 hrs)
 $6''.0 \times 6''.0$
r.m.s = 42 μ Jy/beam
 $S_P = 106$ mJy/beam

WAT ?

core

10"

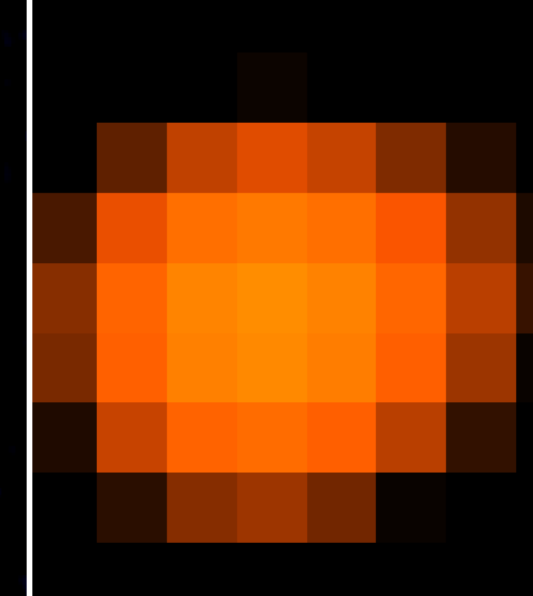


$z=2.06$ $L_R = 2.5 \times 10^{27}$ W/Hz

ILT (48 hrs)
 $0''.47 \times 0''.33$
r.m.s ~ 20 μ Jy/beam
 $S_P = 17$ mJy/beam

core

10"



$z=3.03$ $L_R = 8.5 \times 10^{26}$ W/Hz

LOFAR (72 hrs)
 $6''.0 \times 6''.0$
r.m.s = 50 μ Jy/beam
 $S_P = 73$ mJy/beam

ILT (48 hrs)
 $0''.57 \times 0''.42$
r.m.s ~ 19 μ Jy/beam
 $S_P = 6.0$ mJy/beam

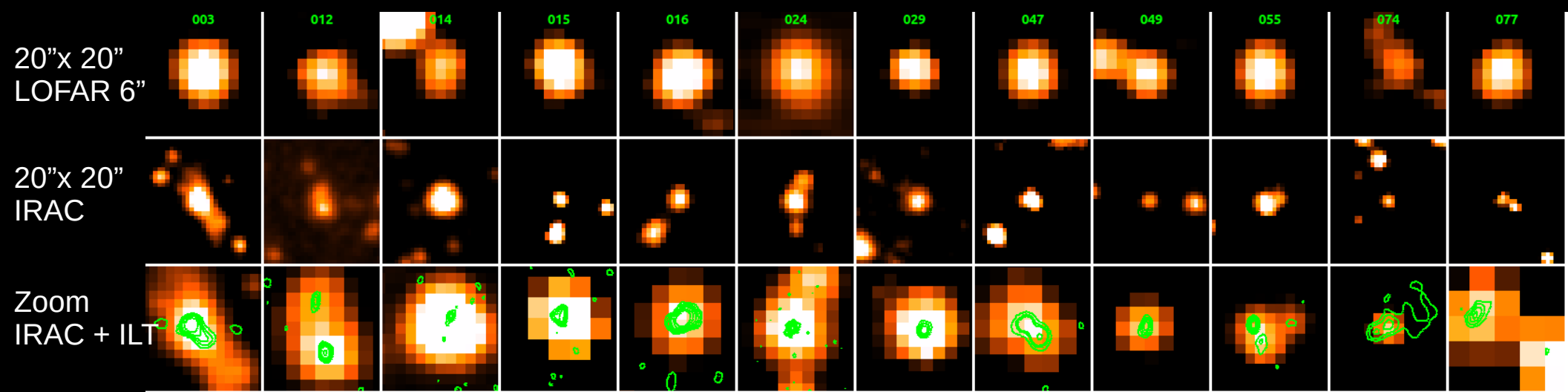
LOFAR (72 hrs)
 $6''.0 \times 6''.0$
r.m.s = 40 μ Jy/beam
 $S_P = 12$ mJy/beam

Exploiting Deep Fields observations with the ILT: bright sub-mm galaxies in the NEP field

| SMM ID | RA IRAC deg | Dec IRAC deg | S 850um mJy | redshift | LIR $\times 10^{39} \text{ W Hz}^{-1}$ | SFR $M_{\odot} \text{ yr}^{-1}$ | Mstar $\times 10^{10} M_{\odot}$ | f_{AGN} |
|--------|----------------|-----------------|----------------|-----------------|---|------------------------------------|-------------------------------------|------------------|
| 3 | 268.18233 | 66.14292 | 23.2 ± 1.9 | 2.89 ± 0.15 | 8.82 ± 1.16 | 1965 ± 309 | 82.7 ± 15.8 | SFG |
| 15 | 267.92028 | 66.80276 | 12.1 ± 2.5 | 2.10 ± 0.80 | 2.73 ± 2.21 | 932 ± 796 | 4.4 ± 1.8 | SFG |
| 12 | 269.33760 | 65.92769 | 11.7 ± 3.2 | 2.59 ± 0.13 | 7.58 ± 0.94 | 2276 ± 312 | 29.7 ± 4.4 | SFG |
| 29 | 268.81288 | 66.73238 | 11.0 ± 1.8 | 3.38 ± 0.19 | 1.98 ± 0.54 | 544 ± 144 | 5.8 ± 1.5 | AGN |
| 16 | 268.19279 | 66.10346 | 10.9 ± 2.9 | 3.21 ± 0.07 | 9.35 ± 0.83 | 2031 ± 235 | 172 ± 18 | AGN/SFG |
| 47 | 268.31280 | 66.82952 | 10.4 ± 1.7 | 3.26 ± 0.63 | 8.21 ± 2.88 | 2037 ± 714 | 40.1 ± 33.9 | AGN/SFG |
| 14 | 269.56415 | 65.86654 | 10.1 ± 4.0 | 1.73 ± 0.09 | 2.57 ± 0.71 | 437 ± 132 | 131 ± 31 | AGN/SFG |
| 55 | 268.69986 | 66.58029 | 10.0 ± 1.8 | 3.13 ± 0.10 | 7.20 ± 0.69 | 1386 ± 133 | 154 ± 15 | AGN/SFG |
| 24 | 270.46358 | 66.57362 | 9.8 ± 2.8 | 2.12 ± 0.16 | 9.20 ± 1.76 | 3137 ± 590 | 38.5 ± 7.3 | SFG |
| 49 | 268.30263 | 66.98022 | 9.7 ± 2.2 | 2.57 ± 0.20 | 6.33 ± 1.74 | 1883 ± 522 | 17.1 ± 5.1 | SFG |
| 74 | 268.32154 | 66.84883 | 9.1 ± 1.7 | 2.99 ± 1.01 | 5.67 ± 2.92 | 1626 ± 870 | 27.7 ± 33.9 | AGN/SFG |
| 77 | 268.23630 | 66.72278 | 9.0 ± 1.8 | 3.57 ± 1.13 | 5.52 ± 3.06 | 1428 ± 814 | 26.0 ± 23.3 | AGN/SFG |

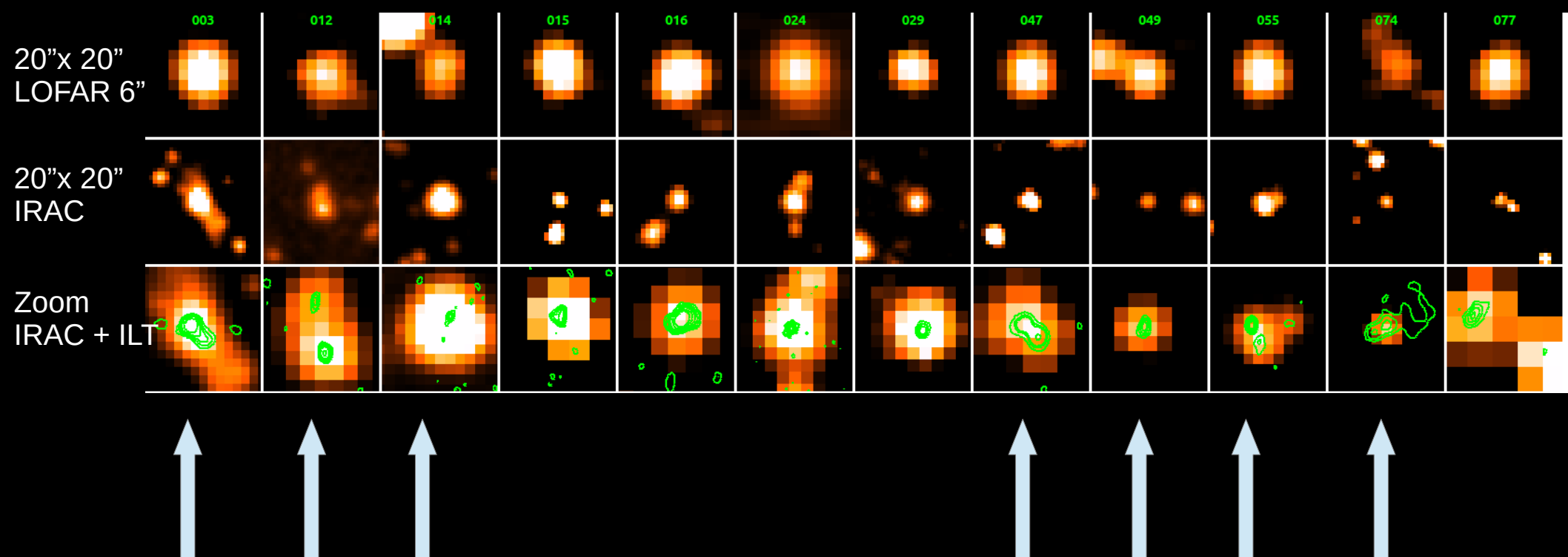
- Selected all SMGs with $S_{850-\mu\text{m}} \geq 9 \text{ mJy}$, $r < 1.2 \text{ deg}$ from field center, and robust SED fit from Shin+ 2022 catalog:
 - 12 objects: $1.7 < z < 3.5$, $\text{SFR} > 1000 M_{\odot}/\text{yr}$
 - 11/12 detected in LOFAR 6" image (72hrs) with $\text{SNR} > 5$ (1/7 with $4 < \text{SNR} < 5$):
 - $0.16 \text{ mJy/b} < S_{6''} < 1.6 \text{ mJy/b}$
 - $\sim 8 \times 10^{24} \text{ W/Hz} < L_{144\text{MHz}} < 5 \times 10^{25} \text{ W/Hz}$

Bright SMGs in the NEP field: Multiplicity



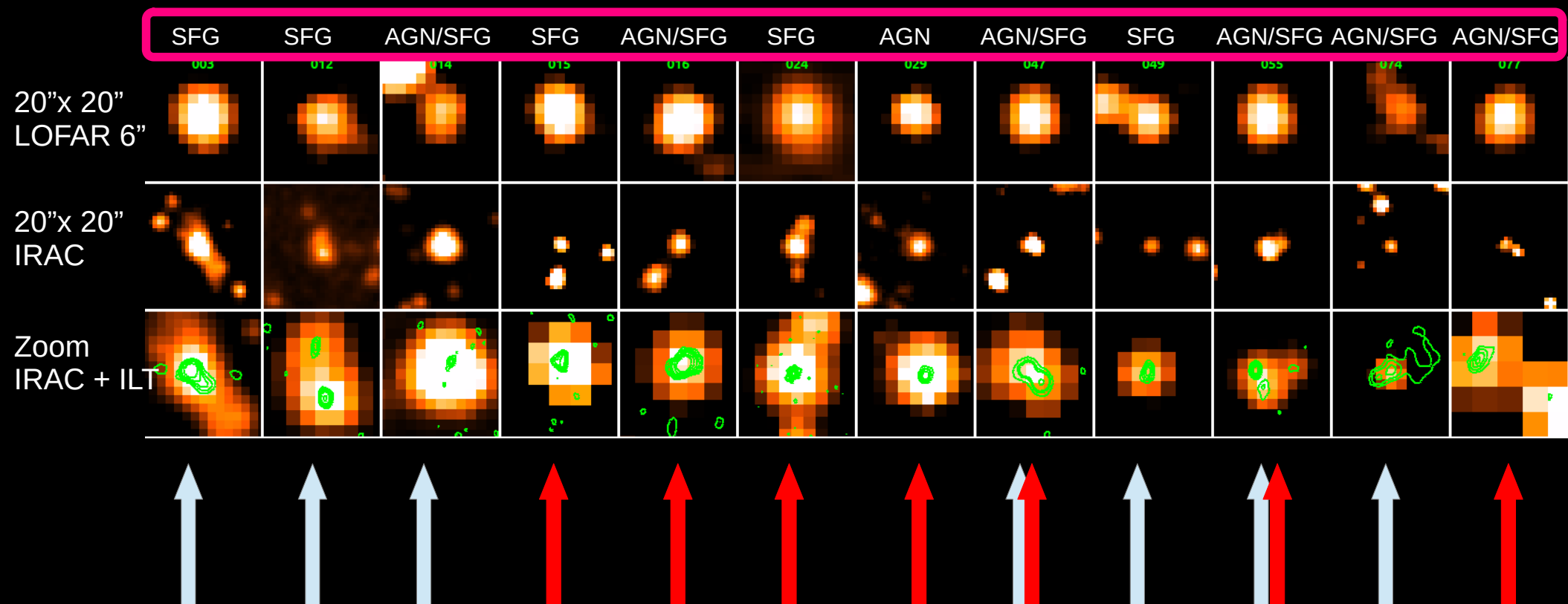
| SMM ID | RA deg | Dec deg | FWHM arcsec | P.A. deg | rms mJy/beam | S_p mJy/beam | S_T mJy | Maj arcsec | Min arcsec | PA deg | $\log T_b$ K |
|--------|-----------|------------|--------------------|-------------|-----------------|-------------------|--------------|---------------|---------------|-----------|-----------------|
| 3a | 268.18213 | 66.14298 | 1.07×0.84 | 109 | 0.026 | 0.155 | 0.467 | 1.56 | 1.14 | 34 | 4.78 |
| 3b | 268.18280 | 66.14323 | | | | 0.303 | 0.421 | 0.75 | 0.42 | 153 | |
| 12a | 269.33762 | 65.92764 | 0.54×0.39 | 174 | 0.013 | 0.112 | 0.180 | 0.45 | 0.24 | 27 | 5.55 |
| 12b | 269.33786 | 65.92823 | | | | 0.072 | 0.121 | 0.80 | 0.1 | 2 | |
| 14 | 269.56387 | 65.86684 | 0.54×0.39 | 173 | 0.013 | 0.075 | 0.176 | 1.11 | 0.1 | 159 | 5.41 |
| 15 | 267.92029 | 66.80301 | 0.38×0.26 | 176 | 0.020 | 0.209 | 0.549 | 0.47 | 0.35 | 5 | 5.86 |
| 16 | 268.19272 | 66.10365 | 0.56×0.41 | 172 | 0.013 | 0.214 | 0.479 | 0.69 | 0.34 | 109 | 5.70 |
| 24 | 270.46381 | 66.57376 | 0.27×0.19 | 179 | 0.026 | 0.305 | 1.152 | 0.43 | 0.33 | 136 | 6.17 |
| 29 | 268.81271 | 66.73252 | 0.58×0.43 | 172 | 0.015 | 0.176 | 0.234 | 0.31 | 0.23 | 102 | 5.93 |
| 47a | 268.31247 | 66.82954 | 0.64×0.47 | 168 | 0.017 | 0.193 | 0.285 | 0.38 | 0.34 | 84 | 5.74 |
| 47b | 268.31287 | 66.82968 | | | | 0.150 | 0.263 | 0.55 | 0.38 | 121 | |
| 49 | 268.30255 | 66.98044 | 0.62×0.47 | 168 | 0.019 | 0.125 | 0.192 | 0.50 | 0.31 | 157 | 5.41 |
| 55a | 268.70044 | 66.58057 | 0.57×0.42 | 172 | 0.015 | 0.231 | 0.323 | 0.37 | 0.26 | 175 | 5.91 |
| 55b | 268.70010 | 66.58025 | | | | 0.073 | 0.264 | 0.99 | 0.63 | 2 | |
| 55c | 268.69882 | 66.58058 | | | | 0.057 | 0.134 | 0.83 | 0.21 | 89 | |
| 74 | 268.32144 | 66.84910 | 3.11×1.66 | 111 | 0.030 | 0.096 | 0.156 | 3.03 | 1.10 | 130 | 4.04 |
| 77 | 268.23682 | 66.72313 | 0.37×0.26 | 176 | 0.018 | 0.105 | 0.390 | 0.69 | 0.34 | 134 | 5.65 |

Bright SMGs in the NEP field: Multiplicity



- Multiple components: 3 (arcsec scale) + 4 (sub-arcsec scale)

Bright SMGs in the EDFN: radio AGN



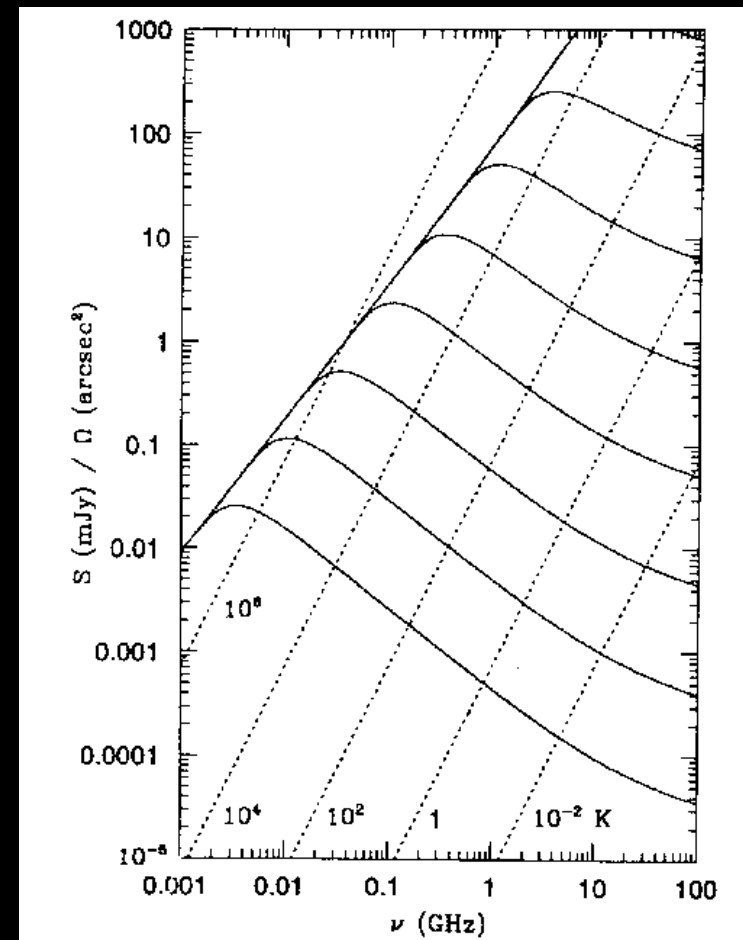
- Brightness Temperature exceeding the limit for star-formation (e.g. Condon 1991): 7 SMGs with $\log(T_b) > 5.6$

T_b as AGN proxy

- Maximum brightness temperature for a normal galaxy with thermal and non thermal emission (Condon 1991):

$$T_b = T_e (1 - e^{-\tau_{\text{ff}}}) \left(1 + 10 \left(\frac{\nu}{1 \text{ GHz}} \right)^{0.1+\alpha} \right)$$

- Normal galaxies have $T_b \leq 10^5$ for $\nu \geq 1 \text{ GHz}$



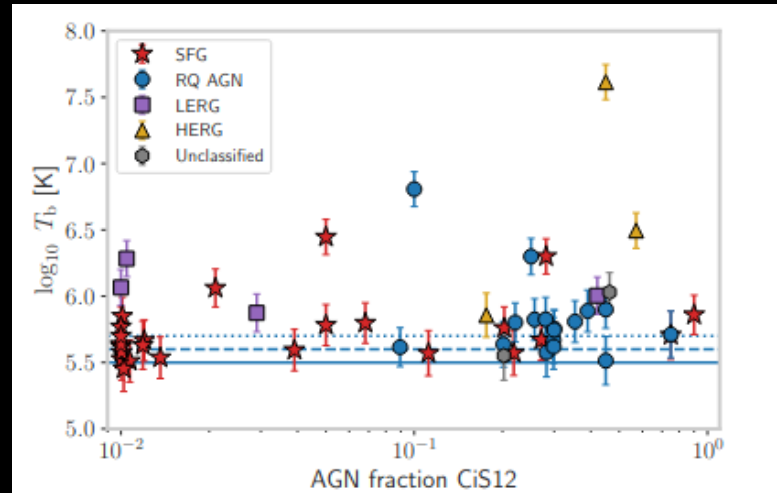
T_b as AGN proxy

- Maximum brightness temperature for a normal galaxy with thermal and non thermal emission (Condon 1991):

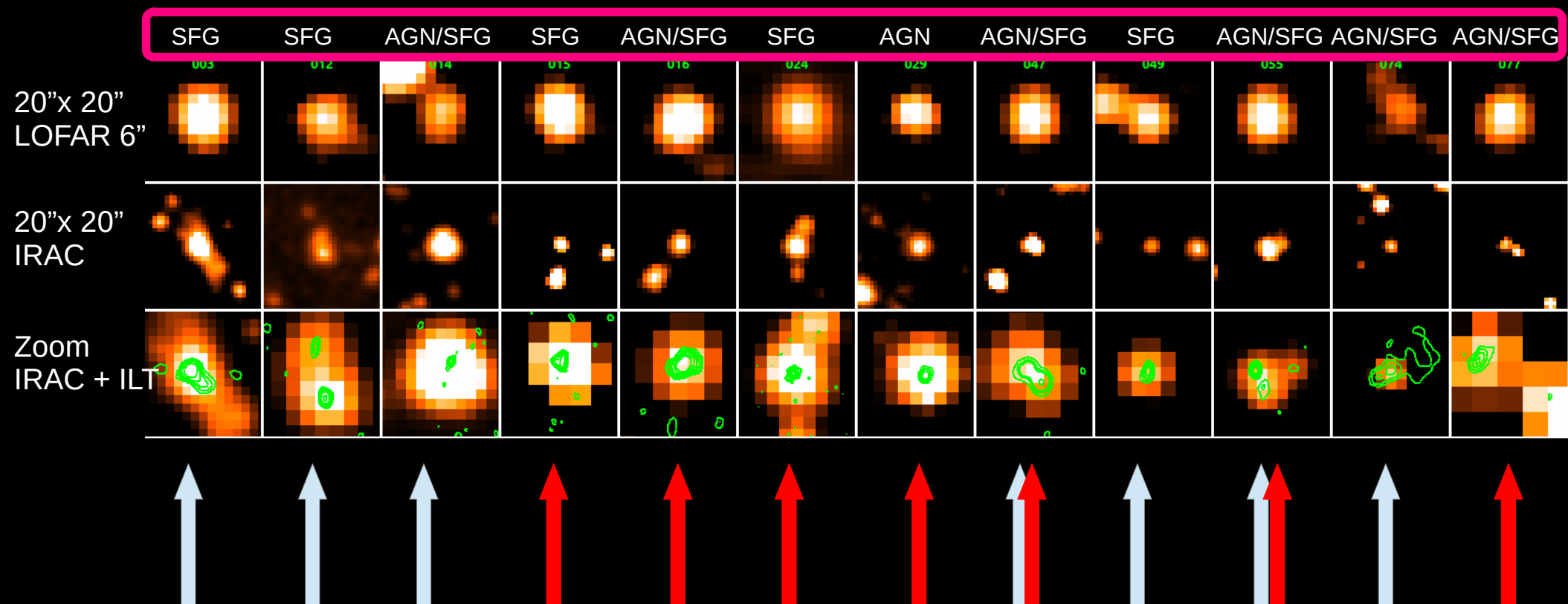
$$T_b = T_e (1 - e^{-\tau_{\text{ff}}}) \left(1 + 10 \left(\frac{\nu}{1 \text{ GHz}} \right)^{0.1+\alpha} \right)$$

- Normal galaxies have $T_b \leq 10^5$ for $\nu \geq 1 \text{ GHz}$
- Sample of ~ 150 HLIRGs in the Lockman Hole (Sweijen+2023, in press), 33% detected with ILT

| Class | N_{obj} | $T_b > 10^{5.7}$ | $T_b > 10^{5.6}$ | $T_b > 10^{5.5}$ |
|--------------|------------------|------------------|------------------|------------------|
| SFG | 25 (103) | 10 | 17 | 24 |
| RQ AGN | 17 | 11 | 15 | 17 |
| LERG | 4 | 4 | 4 | 4 |
| HERG | 3 | 3 | 3 | 3 |
| Unclassified | 2 | 1 | 1 | 2 |
| Total | 51 (103) | 29 | 40 | 50 |

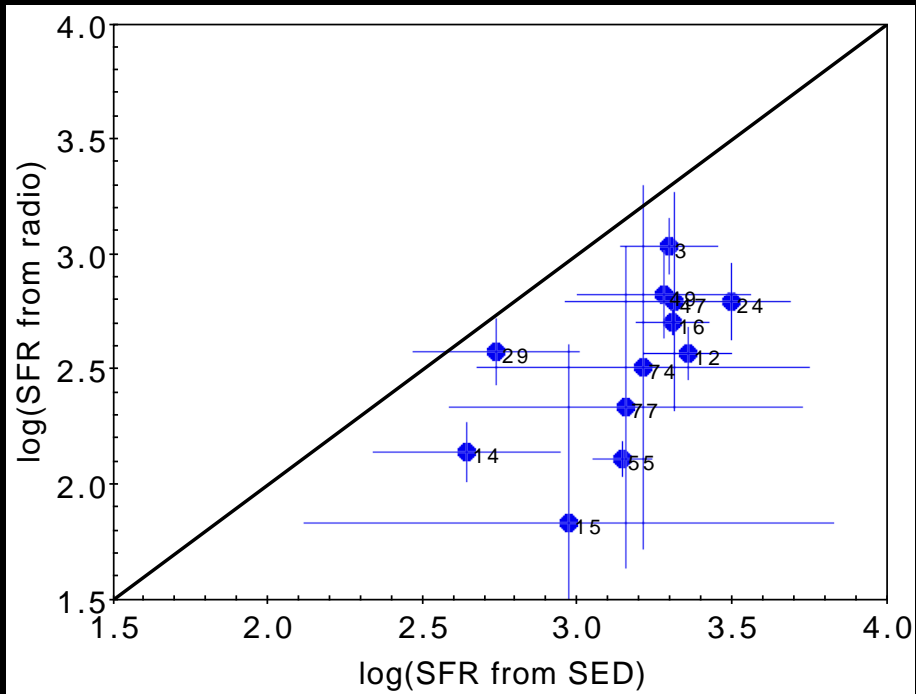


Bright SMGs in the EDFN: radio AGN



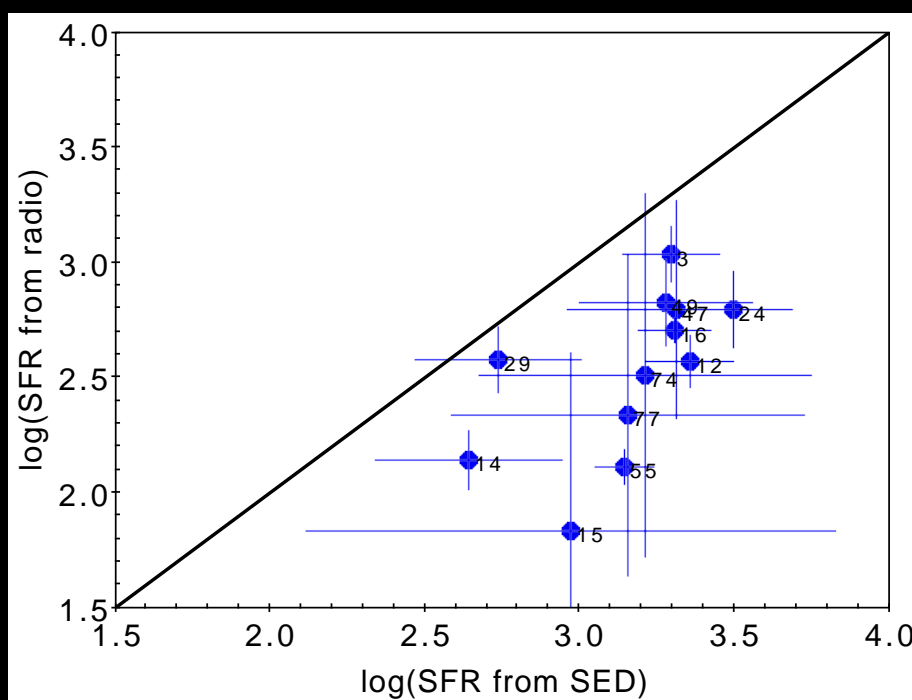
- Brightness Temperature exceeding the limit for star-formation (e.g. Condon 1991): 7 SMGs with $\log(T_b) > 5.6$

Radio vs SED SFRs & main sequence

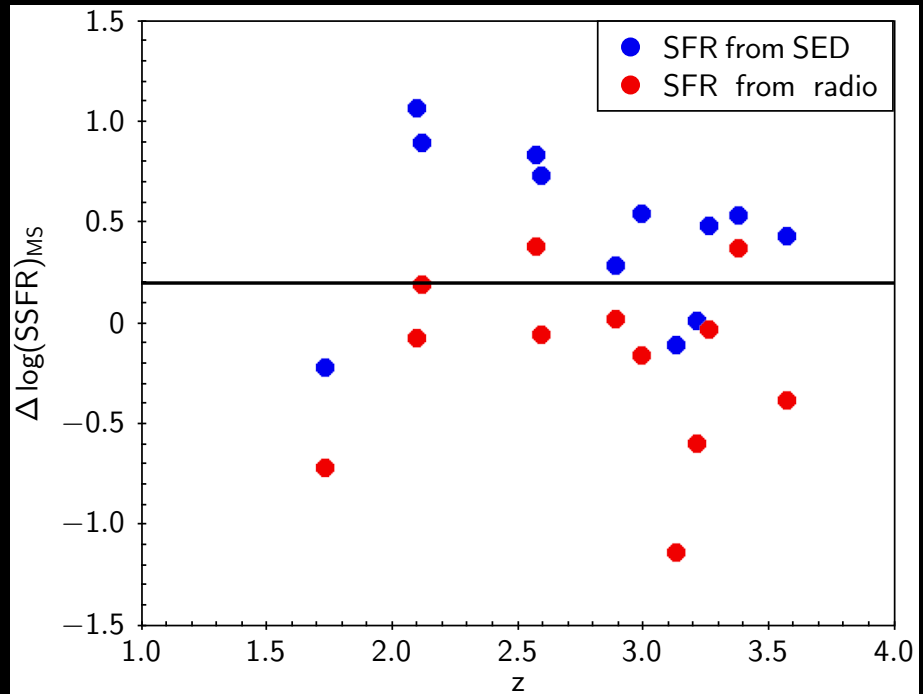


SFR from radio obtained from radio flux at 6'' resolution after subtraction of multiple comp and/or AGN comp: ~5 times lower than that from SED fitting

Radio vs SED SFRs & main sequence



$$\Delta \log (\text{SSFR})_{\text{MS}} = \log [\text{SSFR}_{\text{galaxy}} / \text{SSFR}_{\text{MS}}(M_{\text{star}}, z)]$$



SFR from radio obtained from radio flux at 6" resolution after subtraction of multiple comp and/or AGN comp: ~5 times lower than that from SED fitting

Distance of a galaxy from the star-forming galaxy main sequence (MS) in the SFR-stellar mass plane, removing effects of different stellar mass and z evolution

Summary

- ILT allows imaging the radio sky at 144 MHz with resolution down to $\sim 0.3''$ with average 1σ sensitivity of $\sim 50 \mu\text{Jy}/\text{beam}$ for 8 hrs ($\sim 10-15 \mu\text{Jy}/\text{beam}$ for Deep Fields).
 - Necessary for proper multi- λ identification
 - $<10\%$ of radio sources have sizes $> 10''$, ILT allows to study the details of the remaining 90% (widefield imaging necessary)
- To process a single target with the long-baseline pipeline:
 - e.g. 32-48 cores, Ram $\sim 384 \text{ G}$, disk space $> 15 \text{ T}$
 - 4-8 days of processing, including selfcal and imaging
- A significant fraction of the sky (e.g. LoTSS) has already been observed with the ISs but not processed. Your favorite source might be there !